Application of 3D Printer to the Production of Sound Absorbing Materials and Analysis of Absorption Coefficient Optimization by Taguchi Method

Hao Dong Cheng and Yao Chi Tang*

Systems Engineering and Naval Architecture, National Taiwan Ocean University, Keelung, Taiwan
Email: jasoncheng19991220@gmail.com (H.D.C.); tom@mail.ntou.edu.tw (Y.C.T.)
*Corresponding author

Manuscript received April 10, 2023; revised May 10, 2023; accepted August 23, 2023; published April 8, 2024.

***Abstract*—This study investigated the absorption coefficient of a perforated plate under different design variables and discussed variable optimization. First, a perforated plate sample was printed using stereolithography (SLA) 3D printing, and the absorption coefficient of the sample at a 1/3 octave band was measured using an impedance tube. The design variables included the perforated plate's thickness, perforation rate, and aperture size. We used the Taguchi method for analysis to obtain the optimal combination of variables. The results showed that the perforation rate strongly affected the absorption coefficient in the frequency range of 500 to 6300 Hz. Additionally, the Taguchi method was used to analyze the experimental data because it could quickly find the factors with high influence and the estimated value of the optimal forecast combination.**

***Keywords*—absorption coefficient, optimal perforation rate, perforated plate, taguchi method, 3D printing**

I. Introduction

A. Motivation

With the improved living standards in recent years, the public's tolerance for environmental noise has decreased. Therefore, how to reduce the impact of noise has become an essential topic. Glass fiber is the most commonly used sound-absorbing material, and its absorption capacity for high-frequency noise is outstanding. However, it has a poor absorption coefficient at low and medium frequencies. Therefore, this study used a perforated plate as the outer board of the glass fiber, with the hopes of improving the overall absorption coefficient by using the perforated plate.

B. Experimental Method

3D printing methods are primarily divided into Fused Deposition (FDM) and Stereolithography (STL). In this study, the stereolithography formation method was used to produce samples. Its forming principle is to apply ultraviolet radiation on photosensitive resin to form the required object layer by layer. The advantages of this method are a fast-forming speed and high design elasticity. Therefore, the sample's manufacturing time can be significantly reduced and convenient for testing the confirmatory experiment of the Taguchi method.

The Taguchi method was proposed by Taguchi in the 1950s, and it has been widely used in industrial design [1]. Its primary principle is to construct Taguchi's orthogonal array using the sample average, sample variance, and Signal-to-Noise Ratio (S/N). Then, the mathematical model of each factor can be obtained using Taguchi's orthogonal array. The optimal combination of each factor is then permutated and verified by a confirmatory experiment. The advantage of the Taguchi method is that, compared to full-factorial experiments, it can obtain relatively credible results with fewer experiments through reasonable mathematical methods to achieve an optimal balance between an experiment's costs and its results.

C. Literature Discussion

In 2017, Drabek [2] compared two common testing methods for sound-absorbing materials—impedance or standing wave tube measurement and the reverberation chamber method. This study found that impedance or standing wave tube measurement was more time-saving and cost-effective for understanding a new material's properties. Suhanek *et al.* [3] compared the difference between the transfer function method and the standing wave ratio method. It was found that when using impedance or standing wave tube, the transfer function method for measuring the normal incidence sound absorption coefficient of small samples is much faster than the standing wave ratio method. In 2017, Toyoda *et al.* [4] added glass fiber to the cavity behind a micro-perforated plate and measured the sound absorption rate in a reverberation chamber. The results showed that, with the addition of glass fiber, the sound absorption rate will be higher than that without glass fiber.

In 2021, Sailesh *et al.* [5] fabricated six circular perforations with different section variations using Fused Deposition Modeling (FDM) and placed them into impedance tubes for absorption coefficient and penetration loss tests. In 2020, Xie [6] designed a micro-perforated plate with one micro-perforated hole in each cell of the honeycomb structure. The micro-perforated plate's theoretical model and a Helmholtz resonator were constructed by changing the aperture size and thickness of the micro-perforated plate. Moreover, by comparing it with the measurement results of the actual model in the impedance tube, its influence on the absorption coefficient performance under different variables was obtained. In 2018, Chin *et al.* [7] produced a degradable microperforated plate composed of kenaf fiber and Polylactic Acid (PLA). By measuring the porosity and tensile strength of samples with different mixing ratios, the influence of compositional differences on the sound absorption rate was observed. Zulkifli *et al.* [8] produced a perforated plate made of coconut shell. The sound absorption coefficients of different thicknesses were measured, and it was found that thicker perforated panels have good sound absorption characteristics at both low and high frequencies. These experiments investigated the individual influences of single variables on the experiment. However, they did not discuss

DOI: 10.7763/IJMO.2024.V14.850

the influences on the experiment when there were multiple variables. Since it is challenging to determine which variables have a greater impact, we selected the Taguchi method for testing, because it could obtain the optimal combination of variables with fewer experiments.

This study used the Taguchi method for the experimental design and optimization, and the sound absorption rate was obtained through an impedance tube and the data was analyzed. Different from previous studies that used perforated plates, this study, using Taguchi method, was able to obtain optimal combinations and quantify the importance of factors with fewer runs than traditional experimental designs.

II. Research Methods and Procedures

Fig. 1 illustrates the steps and processes of the Taguchi method used in this study. Sections II and Sections III explain the steps based on the flowchart.

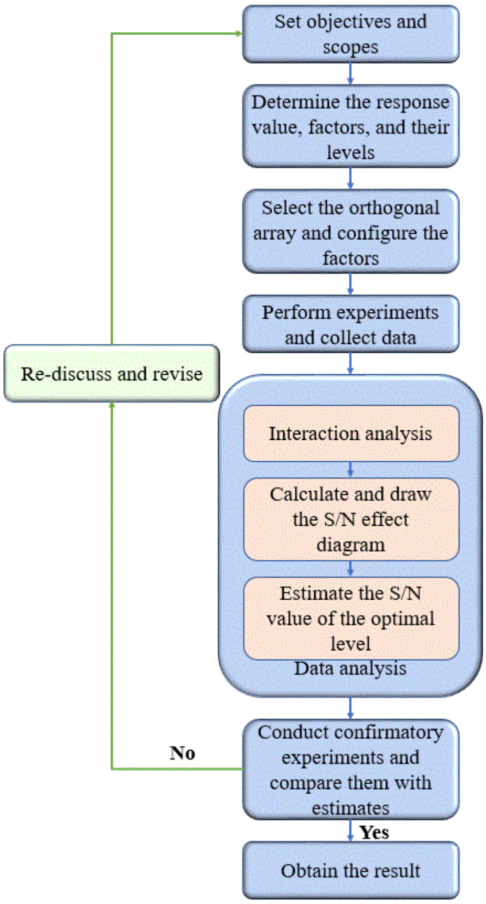

Fig. 1. Flow chart of using the Taguchi method to determine the optimal combination.

A. Objectives and Scope

The objective and scope of this experiment involved establishing a perforated plate with hexagonal holes that was combined with a piece of glass fiber (with a weight of 48 k and a thickness of 20 mm), as shown in Fig. 2.

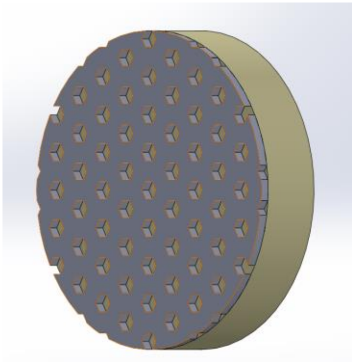

Fig. 2. Schematic diagram of the perforated plate with glass fiber.

This study used the absorption coefficient as the response value to determine the optimal combination of absorption coefficients in the frequency range of 100–6300 Hz. In this research experiment, three signal factors (variables) were set, namely, the perforated plate thickness, the perforation rate, and the aperture diameter. Each factor comprised two levels, as shown in Table 1.

Table 1. Factors and their setting levels

	Level 1	Level 2
Perforated plate thickness	3mm	5mm
Perforation rate	20%	30%
Aperture diameter	5mm	6mm

B. Orthogonal Array Configuration

In this study, two kinds of orthogonal arrays with different experiment times could be selected. If orthogonal arrays of four experiments (L4) and eight experiments (L8) were used, they would correspond to two cases of no interaction between factors and interaction between factors, respectively. Once the selection was complete, we arranged the combination of factors in the experiment. The homeostatic and independent analysis characteristics between the levels needed to be observed to ensure the same number of experiments at each level. While reducing bias (representing the bias caused by not considering the interaction between the factors), a pair of factors with exact duplicate pairs would not be produced, as shown in Tables 2–3.

Table 2. L4 Orthogonal array

Number	Perforated plate thickness	Perforation rate	Aperture diameter
L4-A	3	20%	5
L4-B	3	30%	6
L4-C	5	20%	6
L4-D	5	30%	5

Table 3. L8 Orthogonal array

Number	Perforated plate thickness	Perforation rate	Aperture diameter	Interaction 1	Interaction 2
L8-A	3	20%	5	A	C
L8-B	3	30%	6	A	C
L8-C	3	20%	6	B	D
L8-D	3	30%	5	B	D
L8-E	5	20%	5	A	D
L8-F	5	30%	6	A	D
L8-G	5	20%	6	B	C
L8-H	5	30%	5	B	C

C. Impedance Tube Test

After obtaining the permutations of various experimental factors, the impedance tube and transfer function method were used to measure the absorption coefficient of the sample [9, 10]. According to the ASTM E1050 standard, white noise was generated in the impedance tube. The sound pressure values of different samples at different positions were measured by the impedance tube using a double microphone in the frequency range of 100–6300 Hz, and the measured sound pressure was imported into a spectrum analyzer for analysis. The measurement configuration is shown in Fig. 3.

The transfer function of the impedance tube is shown in Eq. (1):

$$H_{12} = \frac{P_2}{P_1} = \frac{e^{jk_0X_2} + re^{-jk_0X_2}}{e^{jk_0X_1} + re^{-jk_0X_1}} \quad (1)$$

where, H_{12} is the acoustic transfer function, and P_1 and P_2 are the sound pressure measured by the two microphones.

The reflection coefficient was calculated as shown in Eq. (2)

$$R = \frac{e^{-jk_0S} - H_{12}}{H_{12} - e^{jk_0S}} \times e^{2jk_0(l+S)} \quad (2)$$

where, R is the reflection coefficient, S is equal to the distance between the two microphones, and l is the distance from the sample surface to the nearest microphone.

The calculation of the absorption coefficient α is shown in Eq. (3):

$$\alpha = 1 - |R|^2 \quad (3)$$

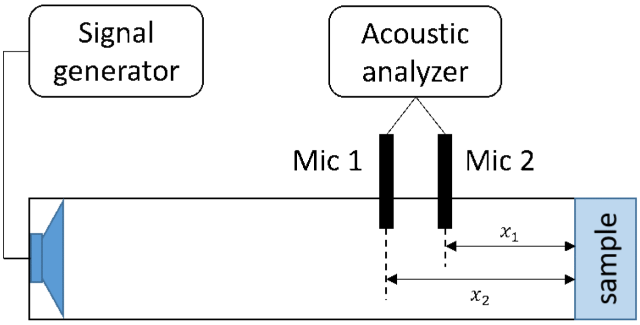

Fig. 3. Configuration diagram of the impedance tube device.

III. Results and Verification

A. Data Analysis Method of area Proportion

The experimental results measured by the impedance tube are shown in Fig. 4–5.

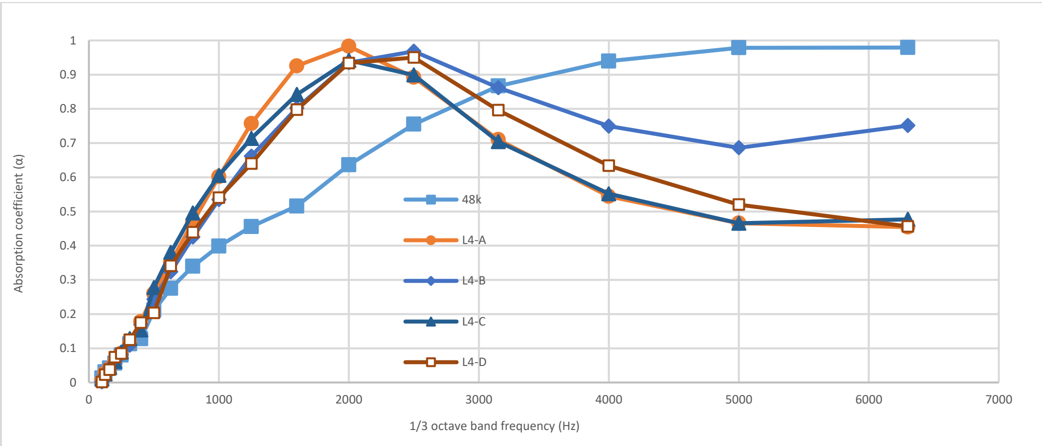

Fig. 4. Absorption coefficient results shown in an L4 orthogonal array.

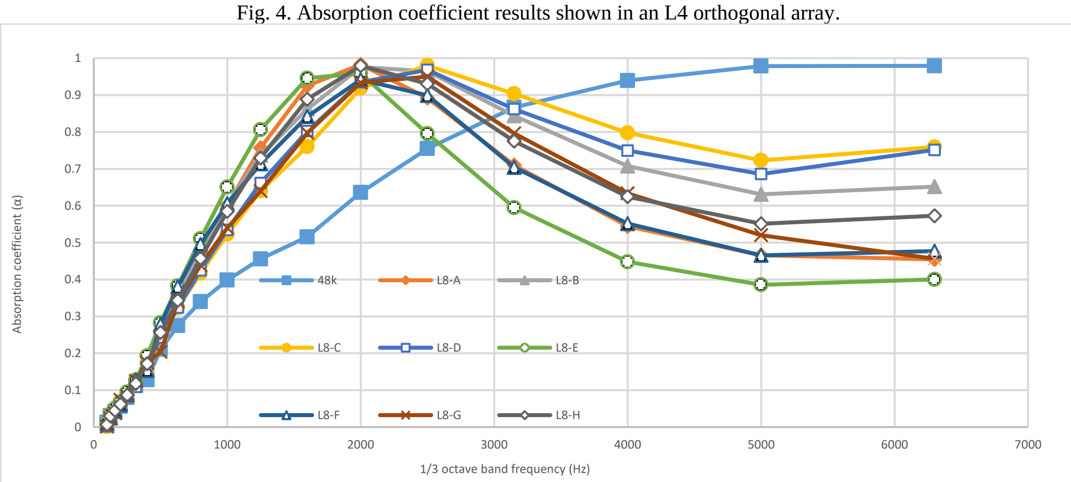

Fig. 5. Absorption coefficient results shown in an L8 orthogonal array.

This study divided the 1/3 octave band into the four categories of low frequency, medium frequency, high frequency, and all pass frequency. Their ranges corresponded to a 1/3 octave band at 100–500 Hz, 500–4000 Hz, 4000–6300 Hz, and 100–6400 Hz, one octave band downwards (500 Hz) and two octave bands upwards (4000 Hz) with 1000 Hz as the center frequency, respectively.

The calculation method for the octave band used is shown in Eq. (4):

$$f_c = 2^{1/6} f_{min} = \frac{f_{max}}{2^{1/6}} \quad (4)$$

where, f_c is the center frequency, f_{min} is the lower limit frequency, and f_{max} is the upper limit frequency.

The upper and lower limits of each center frequency obtained after calculation are shown in Table 4.

Table 4. Upper limit, lower limit and bandwidth of 1/3 octave band

f_c	f_{min}	f_{max}	Band width (Hz)
100	89	112	23
125	111	140	29
160	143	180	37
200	178	224	46
250	223	281	58
315	281	354	73
400	356	449	93
500	445	561	116
630	561	707	146
800	713	898	185
1000	891	1122	232
1250	1114	1403	289
1600	1425	1796	371
2000	1782	2245	463
2500	2227	2806	579
3150	2806	3536	729
4000	3564	4490	926
5000	4454	5612	1158

This study multiplied the frequency band width by the absorption coefficient of the center frequency to calculate the area covered below the curves, as shown in Figures 4 and 5. Next, we calculated the area ratio to perfect sound-absorbing materials (the absorption coefficient of the all-pass frequency was 1), which represented the sound-absorbing capacity of the sample in this experiment at the low, medium, high, and all pass frequencies. The results are shown in Tables 5–6 in two orthogonal arrays.

Table 5. Analysis results of each frequency band in L4 orthogonal array

Result / Sample		L4-A	L4-B	L4-C	L4-D
Low frequency	Sound-absorbing area	64.97	61.21	66.24	59.29
	Area ratio	13.68%	12.89%	13.95%	12.48%
Medium frequency	Sound-absorbing area	2863.12	3083.20	2819.09	2910.43
	Area ratio	70.94%	76.39%	69.85%	72.11%
High frequency	Sound-absorbing area	2863.12	3083.20	2819.09	2910.43
	Area ratio	70.94%	76.39%	69.85%	72.11%
All pass frequency	Sound-absorbing area	4100.15	5006.54	4088.03	4213.71
	Area ratio	58.47%	71.40%	58.30%	60.09%

Table 6. Analysis results of each frequency band in L8 orthogonal array

Result / Sample		L8-A	L8-B	L8-C	L8-D
Low frequency	Sound-absorbing area	64.97	65.25	61.30	61.21
	Area ratio	13.68%	13.74%	12.90%	12.89%
Medium frequency	Sound-absorbing area	2863.12	3125.91	3131.50	3083.20
	Area ratio	70.94%	77.45%	77.59%	76.39%
High frequency	Sound-absorbing area	1706.22	2336.70	2683.63	2584.51
	Area ratio	48.16%	65.95%	75.74%	72.95%
All pass frequency	Sound-absorbing area	4100.15	4841.65	5109.40	5006.54
	Area ratio	58.47%	69.05%	72.87%	71.40%
		L8-E	L8-F	L8-G	L8-H
Low frequency	Sound-absorbing area	71.73	66.24	59.29	64.75
	Area ratio	15.10%	13.95%	12.48%	13.63%
Medium frequency	Sound-absorbing area	2670.91	2819.09	2910.43	2976.16
	Area ratio	66.18%	69.85%	72.11%	73.74%
High frequency	Sound-absorbing area	1445.30	1745.72	1854.57	2051.93
	Area ratio	40.79%	49.27%	52.34%	57.91%
All pass frequency	Sound-absorbing area	3740.30	4088.03	4213.71	4484.77
	Area ratio	53.34%	58.30%	60.09%	63.96%

B. Signal to Noise Ratio and Interactions

The Signal-to-Noise ratio (S/N) represents the robustness of an optimized product or process. A larger S/N value indicates a smaller variation. The S/N ratio can be divided into the quality characteristics of larger-the-better, smaller-the-better, and nominal-the-better, respectively representing the quantity pursued by the response value (for the larger-the-better, the larger the value is, the better). This experiment adopted the quantity characteristic of larger-the-better, which could be calculated as shown in Eq. (5):

$$\mathrm{S/N} = -10 \cdot log\,(\frac{1}{n}\sum_{i=1}^{n}\frac{1}{{y_i}^2}) \qquad (5)$$

where, n is the number of experiments with the same factor and level, and y_i is the experimental value obtained with the same factor and level.

After calculation, the S/N values could be obtained for each level. A larger S/N gap between the same factors but different levels would indicate that the change resulting from changing the factor was more significant, as seen in and Table 6–7, as well as Fig. 6 and. Additionally, the L4 and L8 orthogonal arrays indicated the importance of the factors to the response values.

Table 7. S/N Values of each factor in the L4 orthogonal array and their difference

		Thickness			**Perforation Rate**			**Aperture Diameter**		
		3mm	5mm	Differ-ence	20%	30%	Differ-ence	5mm	6mm	Difference
Low frequency	Thickness	−8.630	−8.846	**0.215**						
	Perforation rate				−8.838	−8.638	**0.201**			
	Aperture diameter							−8.647	−8.829	**0.182**
Medium frequency	Thickness	−1.300	−1.371	**0.071**						
	Perforation rate				−1.456	−1.216	**0.239**			
	Aperture diameter							−1.407	−1.265	**0.142**
High frequency	Thickness	−2.491	−2.592	**0.101**						
	Perforation rate				-2.992	-2.090	**0.902**			
	Aperture diameter							−2.773	−2.309	**0.463**
All pass frequency	Thickness	−1.969	−2.076	**0.107**						
	Perforation rate				−2.271	−1.775	**0.496**			
	Aperture diameter							−2.136	-1.910	**0.226**

Table 8. S/N Values of each factor in the L8 orthogonal array and their difference

		Thickness			**Perforation Rate**			**Aperture Diameter**		
		3mm	5mm	Difference	20%	30%	Differe-nce	5mm	6mm	Difference
Low frequency	Thickness	−8.763	−8.614	**0.149**						
	Perforatio n rate				−8.695	−8.682	**0.012**			
	Aperture diameter							−8.601	−8.777	**0.176**
Medium frequency	Thickness	−1.218	−1.524	**0.305**						
	Perforatio n rate				−1.451	−1.290	**0.161**			
	Aperture diameter							−1.444	−1.298	**0.147**
High frequency	Thickness	−1.889	−3.038	**1.149**						
	Perforatio n rate				−2.771	−2.156	**0.615**			
	Aperture diameter							−2.702	−2.225	**0.478**
All pass frequency	Thickness	−1.694	−2.306	**0.612**						
	Perforatio n rate				−2.162	−1.839	**0.323**			
	Aperture diameter							−2.116	−1.885	**0.231**

In the ideal Taguchi experiment, all factors are linear and independent of each other. This means that Factor A will not change its linear trend due to the difference of Factor B (i.e., there is no interaction). However, in an actual situation, factors often interfere with each other (i.e., there is an interaction). Regarding the interaction, there will be a deviation in the final verification. To determine the interaction between factors in this study, interaction analysis was required. The results are shown in Fig. 8.

As shown in Fig. 8, if the line segments intersected or were about to intersect, it would mean there was an interaction between two factors. To eliminate the deviation caused by such interaction, the horizontal axis of the orthogonal array needed to consider individual factors and establish new combinations of interacting factors. Therefore, in the case of interaction, the L8 orthogonal array with a higher degree of freedom would be used; i.e., Table 1 would be converted to Table 2.

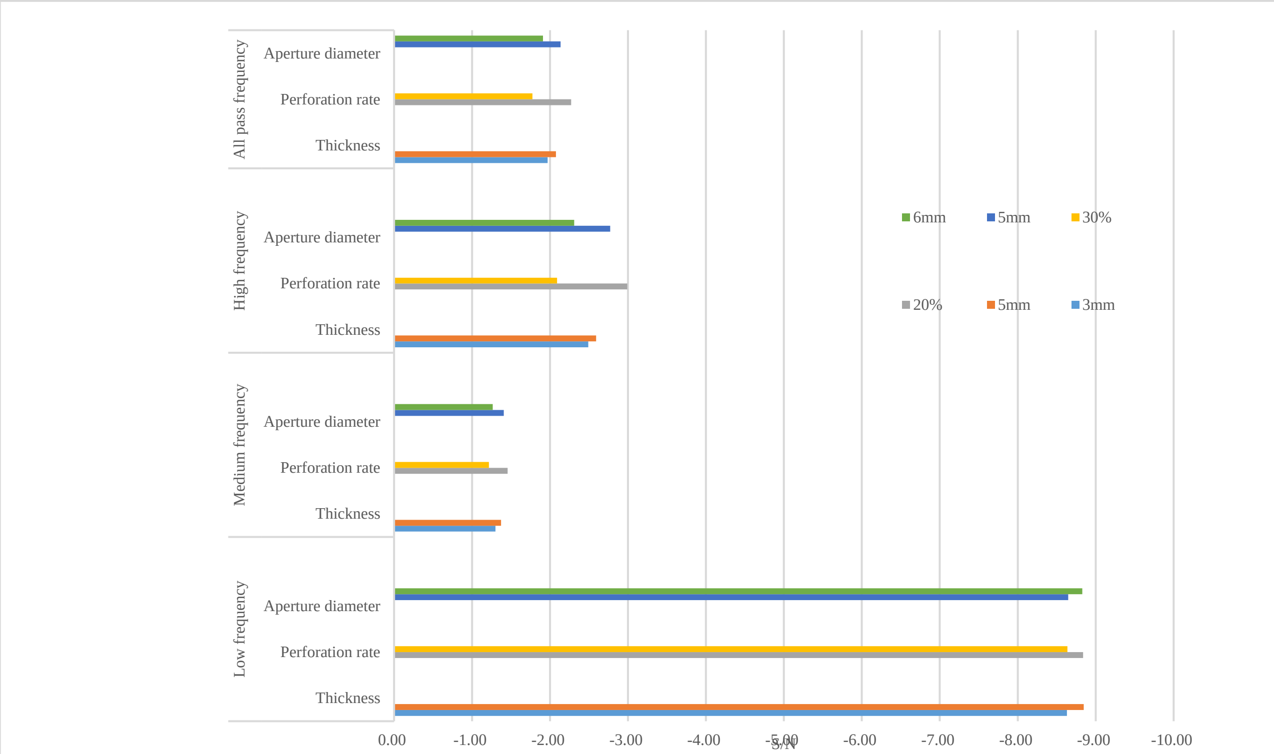

Fig. 6. S/N Effect of L4 Orthogonal Array.

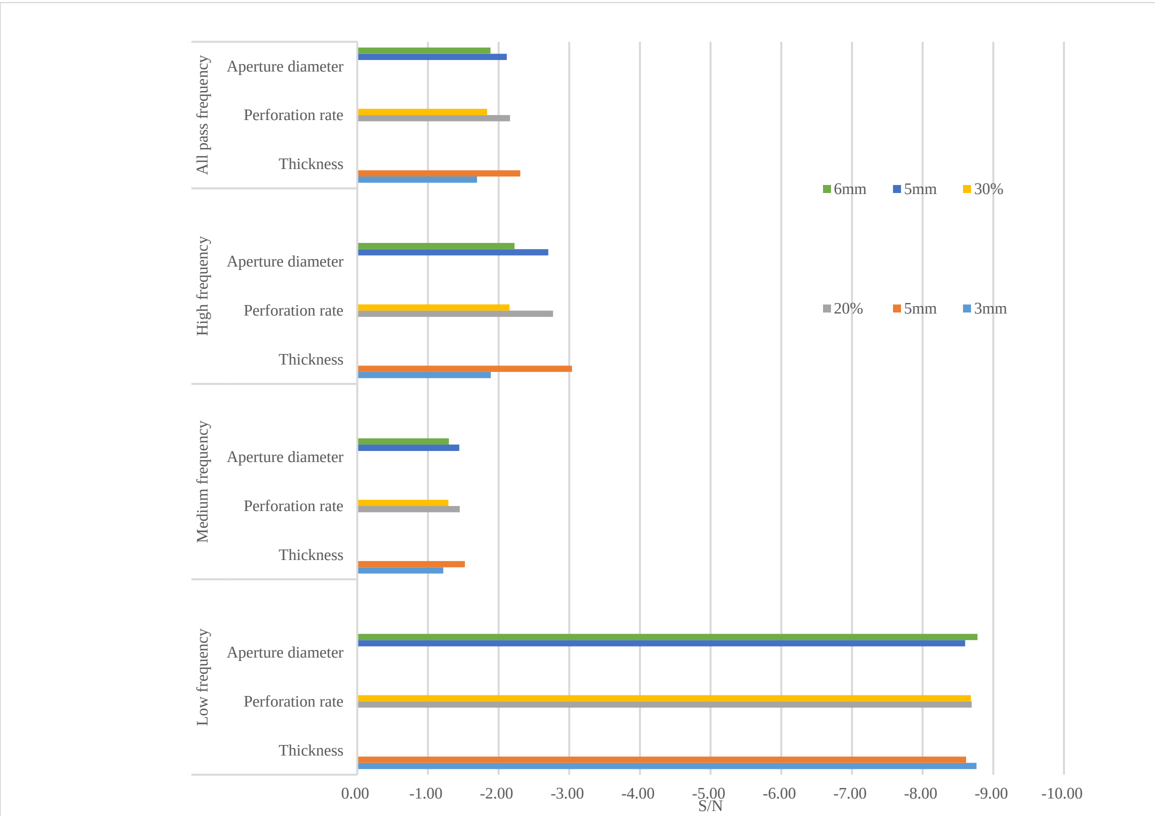

Fig. 7. S/N Effect of L8 orthogonal array.

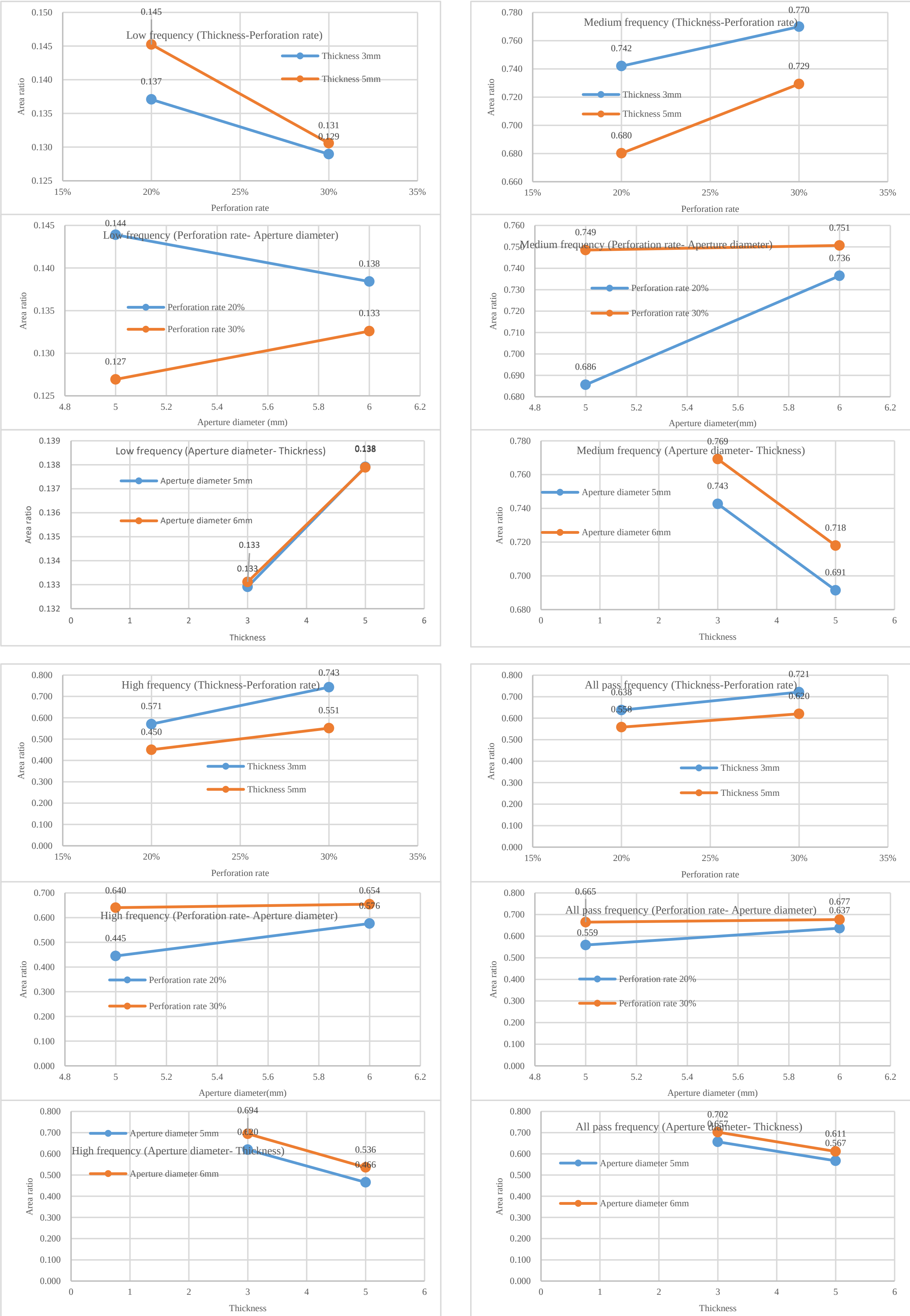

Fig. 8. Interactions of sound absorption in all frequency bands.

C. Orthogonal Array with Interactions

The combination factors with interaction were selected from Fig. 8, including perforation rate * aperture diameter, aperture diameter * thickness, thickness * perforation rate under the low frequency, and the perforation rate and aperture diameter under the medium frequency, high frequency, and all pass frequency. Then, the low frequency, medium frequency, high frequency and all pass frequency were corrected to obtain the new L8 orthogonal arrays of Tables 9 and 10.

Table 9. Corrected L8 orthogonal array under the low frequency

Number	**Thickness**	**Perforation rate**	**Aperture diameter**	**Perforation rate * aperture diameter**	**Aperture diameter * thickness**
L8-A	3	20%	5	A	C
L8-B	3	30%	6	A	C
L8-C	3	20%	6	B	D
L8-D	3	30%	5	B	D
L8-E	5	20%	5	A	D
L8-F	5	30%	6	A	D
L8-G	5	20%	6	B	C
L8-H	5	30%	5	B	C

Table 10. Corrected l8 orthogonal array under the medium frequency, high frequency, and all pass frequency

Number	**Thickness**	**Perforation rate**	**Aperture diameter**	**Perforation rate * aperture diameter**
L8-A	3	20%	5	A
L8-B	3	30%	6	A
L8-C	3	20%	6	B
L8-D	3	30%	5	B
L8-E	5	20%	5	A
L8-F	5	30%	6	A
L8-G	5	20%	6	B
L8-H	5	30%	5	B

Through the corrected orthogonal array, the S/N value of the new combination generated by the interaction could be obtained (as shown in Table 11). The effect diagram of the composition of the S/N difference value is shown in Fig. 9:

Table 11. S/N Values generated by interaction and their differences

		Perforation rate * aperture diameter			**Aperture diameter * thickness**		
		A	**B**	**Differ-ence**	**C**	**D**	**Dif-fere-nce**
Low frequency	Perforation rate * aperture diameter	-8.507	-8.871	**0.364**			
	Aperture diameter * thickness				−8.738	−8.639	**0.099**
Medium frequency	Perforation rate * aperture diameter	−1.488	−1.254	**0.234**			
High frequency	Perforation rate * aperture diameter	−2.987	−1.940	**1.047**			
All pass frequency	Perforation rate * aperture diameter	−2.253	−1.748	**0.505**			

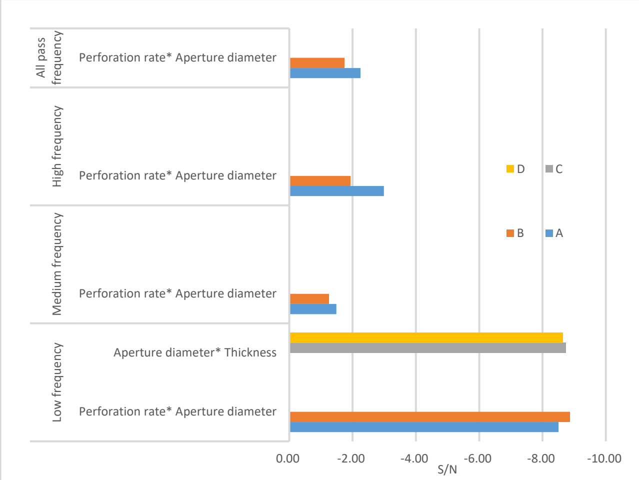

Fig. 9. S/N Effect Diagram of the Interaction.

D. Confirmatory Experiment

By conducting the S/N and interaction experiments, we could determine the most influential factors for the experiment. Furthermore, the optimal combination could be found according to the larger S/N, as shown in Table 12 and Table 13.

Table 12. The optimal combination of factors in each frequency band in the L4 orthogonal array

	Low frequency	**Medium frequency**	**High frequency**	**All pass frequency**
Thickness	3mm	3mm	3mm	3mm
Perforation rate	30%	30%	30%	30%
Aperture diameter	5mm	6mm	6mm	6mm

Table 13. The optimal combination of factors in each frequency band in the L8 orthogonal array

	Low frequency	**Medium frequency**	**High frequency**	**All pass frequency**
Thickness	3mm	3mm	3mm	3mm
Perforation rate	30%	30%	30%	30%
Aperture diameter	5mm	6mm	6mm	6mm
Perforation rate * aperture diameter	20%×5mm	30%×6mm	30%×6mm	30%×6mm
Aperture diameter * thickness	6mm×5mm			
Thickness * perforation rate	5mm×20%			

The S/N obtained by combining the optimal factor levels was compared with the S/N of the actual experiment to determine whether they were close to verifying the accuracy of the experiment. Additionally, when estimating the S/N of the optimal combination, to avoid overestimation, the combination with relatively high influence was selected for calculation, and the factors with low influence were combined as errors. The calculation method of the estimated S/N is shown in Eq. (6).

$$S/N = A_i + B_j + C_k + \cdots + (n-1)\overline{S/N} \quad (6)$$

A_I, B_J, C_K denote the optimal level of each factor, which also contains the combination of interactions. n is the number of selected factors, and $\overline{S/N}$ represents the average of all S/N.

In this experiment, when S/N was estimated, the most influential two to three groups of factors were selected for calculation. The estimated S/N values were calculated (as shown in Table and Table). The estimated S/N was compared with the experimental value, and the difference is shown in Tables 14–15.

Table 14. Estimated S/N values in the L4 orthogonal array

	Low frequency	Medium frequency	High frequency	All pass frequency
Thickness	–8.630	–1.300	–2.491	–1.969
Perforation rate	–8.638	–1.216	–2.090	–1.775
Aperture diameter	–8.647	–1.265	–2.309	–1.910
S/N average	–8.73808	–1.33594	–2.5411	–2.02293
Factor quantity adopted	3	3	3	3
Estimated S/N	**–8.4389**	**–1.110**	**–1.808**	**–1.608**

Table 15. Estimated S/N in the L4 Orthogonal Array, Estimated S/N of Combination Experiment and the Difference Between Them

	Low frequency	Medium frequency	High frequency	All pass frequency
Estimated S/N	–8.439	–1.110	–1.808	–1.608
Actual S/N	–8.893	–1.170	–1.370	–1.463
Difference	**0.453**	**0.060**	**0.438**	**0.145**

E. Results and Discussion

According to Tables 16 and 17, when the perforated plate is at medium frequency, high frequency and all pass frequency, the S/N difference of the perforated plate thickness is about 1.9 times the perforation rate and 2.5 times the aperture diameter. When the interaction is considered, the S/N difference of thickness is about 1.1 times the perforation rate * aperture diameter, and it could distinguish the influence degree of each factor in this experiment.

Table 16. Estimated S/N values in the L8 orthogonal array

	Low frequency	Medium frequency	High frequency	All pass frequency
Thickness	–8.614	–1.218	–1.889	–1.694
Perforation rate	N/A	–1.290	N/A	–1.839
Aperture diameter	–8.601	N/A	N/A	N/A
Perforation rate * aperture diameter	–8.383	–1.246	–1.871	–1.702
Aperture diameter * thickness	N/A	N/A	N/A	N/A
S/N average	–8.689	–1.371	–2.464	–2.000
Number of selected factors	3.000	3.000	2.000	3.000
Estimated S/N	**–8.220**	**–1.013**	**–1.297**	**–1.235**

Table 17. estimated S/N in the L8 orthogonal array, estimated S/N of combination experiment and the difference between them

	Low frequency	Medium frequency	High frequency	All pass frequency
Estimated S/N	–8.220	–1.013	–1.297	–1.235
Actual S/N	–8.640	–1.169	–1.370	–1.463
Difference	**0.419**	**0.157**	**0.073**	**0.228**

According to the research results, the difference between the estimated S/N and the actual S/N would be more accurate at higher frequencies. Table 18 shows the mean difference between the L4 estimated value and that the actual S/N was 0.274. The variance was 0.030. The mean difference between the L8 estimated value and the actual S/N was 0.219. The variance was 0.0163. Both the mean difference of the L8 and the variance were small, indicating that experiments with interaction could estimate the actual experimental value more accurately.

Regarding whether the estimated combination was the optimal combination, we found that the actual optimal combination was not the estimated one. However, the S/N values of the actual optimal combination at medium frequency, high frequency, and all pass frequency were similar to the real S/N values of the estimated combination, as shown in Table 18. The main reason for the deviation is that the factor "thickness" also interacts with the factor "perforation rate * aperture diameter."

Table 18. Comparison between the S/N of the estimated combination in the experiment and the S/N of the actual optimal combination

	Low frequency	Medium frequency	High frequency	All pass frequency
S/N of the estimated combination in the experiment	–8.640	–1.169	–1.370	–1.463
S/N of the actual optimal combination	–8.210	–1.102	–1.206	–1.375
S/N difference	0.430	0.068	0.163	0.088

IV. Conclusion

This study used the Taguchi method to explore the characteristics of sound-absorbing materials with frequencies ranging from 100 to 6300 Hz, and their influence on the absorption coefficient was further discussed by changing different variables. The following conclusions were drawn.

1) In the medium and high-frequency bands, the two most influential factors were the thickness and the perforation rate * aperture diameter in interaction. Glass fiber typically absorbs high-frequency sound. When the plate thickness was thin and the perforation rate and aperture area were large, medium- and high-frequency sounds could more easily penetrate the perforated plate and be absorbed.
2) Regarding the accuracy, it could obtain relatively correct results for a single factor or factors with high influence. If more complete calculations of interactions or several experiments could be made, more precise

influences and optimal combinations of experiments could be obtained.

3) Regarding the time-saving benefits, the interaction between factors and the influence of specific variables on the experiments could be obtained through fewer experiments.
4) Due to the few settings of the experimental factors and level numbers in this study, the number of experiments increased for interaction reached the same number as that of the full-factorial experiment. Without interaction, the number of experiments was reduced by half. Although less precise, we could still obtain the same optimal combination as experiments with interaction. We also reduced the number of experiments with interactions by increasing the number of factors or levels.
5) According to the above-mentioned conclusions, besides the full-factorial experiment, the Taguchi method could also be used as an effective way to reduce the experimental cost while maintaining accuracy when designing experiments with more factors and levels.

In this study, the experiment of perforated plate was designed by the Taguchi method. The results showed that this method had certain accuracy and could quantify the importance of each factor. Therefore, the Taguchi method could be helpful for other research projects that contain more factors and levels.

Conflict of Interest

The authors declare no conflict of interest

Author Contributions

H.D. Cheng conducted the research and analyzed the data; Y.C. Tang review and provide suggestions about the study; H.D. Cheng, Y.C. Tang wrote the paper; all authors had approved the final version.

Acknowledgment

Hao Dong Cheng thanks professor Guo Hao Li for giving advice on Writing and reviewing paper.

References

[1] H. H. Lee, *Taguchi Methods: Principles and Practices of Quality Design*, 4th ed.: Gau Lih Book, 2020.

[2] P. Drabek, "Comparison of two internationally recognized methods for determining the sound absorption coefficient," in *Proc. MATEC Web of Conferences*, vol. 125, 2017.

[3] M. Suhanek, K. Jambroši, and M. Horvat, "A comparison of two methods for measuring the sound absorption coefficient using impedance tubes," in *Proc. 50th International Symposium ELMAR-2008*, 10-12 September 2008.

[4] M. Toyoda, K. Sakagami, M. Okano, T. Okuzono, and E. Toyoda, "Improved sound absorption performance of three-dimensional MPP space sound absorbers by filling with porous materials," *Applied Acoustics*, vol. 116, 2017.

[5] R. Sailesh, L. Yuvaraj, Jeyaraj Pitchaimani, M. Doddamani, L. Babu M. Chinnapandi, "Acoustic behaviour of 3D printed bio-degradable micro-perforatedpanels with varying perforation cross-sections," *Applied Acoustics*, vol. 174, 2021.

[6] S. C. Xie, D. Wang, Z. J. Feng, and S. C. Yang, "Sound absorption performance of microperforated honeycomb metasurface panels with a combination of multiple orifice diameters," *Applied Acoustics*, vol. 158, 2020.

[7] D. D. V. S. Chin, M. N. B. Yahya, N. B. C. Din, and P. Ong, "Acoustic properties of biodegradable composite micro-perforated panel (BC-MPP) made from kenaf fibre and polylactic acid (PLA)," *Applied Acoustics*, vol. 128, 2018.

[8] R. Z. Zulkarnain and M. J. M. Nor, "Noise control using coconut coir fiber sound absorber with porous layer backing and perforated panel," *American Journal of Applied Sciences*, no. 7, no. 2, pp. 260–264, 2010.

[9] A. F. Seybert, "Notes on absorption and impedance measurements," *Astm E1050*, pp. 1–6, 2010.

[10] *Standard Test Method for Impedance and Absorption of Acoustical Materials Using a Tube, Two Microphones and a Digital Frequency Analysis System*, ASTM Standard E1050.